PHYSICAL REVIEW A VOLUME 36, NUMBER 9 NOVEMBER 1, 1987

Renormalization of an inverse-scattering theory for discontinuous profiles

Arthur K. Jordan and H. Douglas Ladouceur
Naval Research Laboratory, Washington, D.C. 20375
(Received 1 December 1986)

A renormalized solution that is based upon the exact inversion theories of Gel'fand, Levitan, and Marchenko has been developed by using a multiple-scales analysis. Our previous theory [J. Opt. Soc. Am. A **2**, 1916 (1985)] for the inverse-scattering problem for inhomogeneous, continuously varying regions has been extended to include discontinuities in the dielectric permittivity. A singular perturbation method has been used to obtain a uniformly valid expression for the electric field within the dielectric region. The advantage of the multiple-scales analysis of the interior electric field is that it rigorously indicates the dielectric region over which the weak-scattering or high-frequency approximation is valid. Furthermore, it is an effective renormalization technique that is physically motivated by the requirement of energy conservation and that allows a systematic investigation of the various scales associated with the inverse problem. The singular perturbation method for the solution of the inverse problem associated with the electromagnetic reflection data from a discontinuous dielectric region utilizes the high-frequency Born approximation to determine the magnitude of the discontinuity in the neighborhood of the origin. The method used for reconstructing discontinuous profiles is also appropriate for the reconstruction of profiles with turning points. The theory is demonstrated by two examples.

INTRODUCTION

Inverse-scattering theories provide methods for reconstructing the physical properties of unknown objects from information contained in scattering data. If the scattering data can be represented by an analytic scattering matrix, i.e., perfect data over an infinite bandwidth in wave-number space, then mathematically exact inverse theories[1,2] can be used to reconstruct the scattering potential or the equivalent profile of refractive index. However, all practical scattering data are limited and, in any case, calculations based upon exact theories can prove to be formidable. Recourse must then be made to approximate inverse theories that are valid for restricted physical models and limited data sets, for example, weak-scattering (Born) conditions[3] and high-frequency data.[4] The approximately reconstructed refractive-index profiles will have limited validity due to divergent terms in the perturbation expansion for the reflected fields. These secular terms can be effectively summed by using a renormalization method first introduced by Rayleigh[5] to calculate the reflection of light from a stratified medium.

A renormalized inversion theory (Refs. 6 and 7, hereafter referred to as I and II) has been developed that is equivalent to a second-order regular perturbation solution[8] of the exact Gel'fand-Levitan-Marchenko (GLM) integral equation for the inverse-scattering problem. Calculations based upon this theory have accurately reconstructed profiles with an increased radius of convergence in the wave-number domain compared to the Born approximation. The renormalized inversion theory assumed that the dielectric profile was a spatially continuous, slowly varying function of position, had no turning points, and was dispersionless. Under these assumptions, the approximate expression for the electric field within the dielectric region can be derived by the method of multiple scales,[9] which is a perturbation technique equivalent to a renormalization of the electric field. In practice, the field renormalization is accomplished by denying the secular growth of the field amplitude in the higher-order perturbation approximations. The denial of secular growth is physically motivated by the requirement of electromagnetic energy conservation within the dielectric. In the lowest-order approximation the renormalized field is equivalent to the Wentzel-Kramers-Brillouin (WKB) approximation.

In this paper the renormalized inversion theory for smoothly varying profiles will be extended to discontinuous profiles by using singular perturbation theory. Since any finite structure will always present a discontinuity to an incident electromagnetic wave, this generalization is both practical and necessary. To demonstrate this technique, Maxwell's equations within the dielectric region are first reduced to a Helmholtz equation, which in the high-frequency limit is a singular perturbation problem. The general solution is derived by the method of multiple scales and is compared with a solution obtained by an extended WKB approximation. The resulting electric field within the dielectric region is represented by a composite expansion which is bounded throughout the entire interior region. Under the assumptions of our model, the calculations demonstrate that the phase and amplitude of the electromagnetic wave can be regarded as slowly varying functions of position in the region away from the discontinuity. The solution in this region is analogous to the outer solution of boundary-layer theory.

In the neighborhood of the discontinuity, the phase of the field is highly oscillatory; the solution in this region is analogous to the inner solution of boundary-layer theory. However, since the phase function is complex, the inner solution does not decay away from the discontinuity but propagates into the interior as a high-frequency wave. This high-frequency propagation or global breakdown of the inner solution does not pose a problem for the extended inversion algorithm. The Riemann-Lebesgue lemma[10] guarantees that the inner solution does not contribute to the complex reflection coefficient in the outer region. In the neighborhood of the discontinuity, the inner solution can be reduced to the Born approximation for the electric field.

The magnitude and local behavior of the dielectric profile function and its derivatives in the neighborhood of the discontinuity can be accurately determined by a Fourier transform of the complex reflection coefficient. The outer approximation for the electric field provides a kernel to reconstruct the dielectric profile in the assumed slowly varying region. The regional dielectric profiles can then be combined to provide a uniform reconstruction of the entire dielectric profile.

RENORMALIZED INVERSION THEORY FOR CONTINUOUS PROFILES

The physical model considered here is the reflection of perpendicularly polarized, time-harmonic plane waves with wave number k incident at an angle θ_0 on an inhomogeneous region with permittivity $\epsilon(k,z)$, as shown in Fig. 1. The scattering data can be represented by the complex reflection coefficient $r(k,\theta_0)$ so that the inverse problem is to reconstruct the dielectric permittivity profile relative to free space,

$$\epsilon_r(k,z)=\epsilon(k,z)/\epsilon_0, \quad \epsilon_0\approx(1/36\pi)\times 10^{-9}\ \mathrm{F}/m$$

from information contained in $r(k,\theta_0)$.

The total electric field in free space ($z<0$) is

$$E_y(x,z,k,\theta_0)=[\exp(ikz\cos\theta_0)+r(k,\theta_0)\exp(-ikz\cos\theta_0)]\times\exp(ikx\sin\theta_0)\ . \tag{1}$$

The electric field E_y within the dielectric satisfies the scalar Helmholtz equation

$$\frac{\partial^2 E_y}{\partial x^2}+\frac{\partial^2 E_y}{\partial z^2}+k^2\epsilon_r(k,z)E_y=0\ . \tag{2}$$

Since E_y must be continous for all x across the interface, a solution to Eq. (2) has the form

$$E_y=\psi(z,k,\theta_0)\exp(ikx\sin\theta_0)\ , \tag{3}$$

where the scalar field amplitude $\psi(z,k,\theta_0)$ satisfies the one-dimensional Helmholtz equation

$$\frac{d^2\psi}{dz^2}+k^2U^2(k,z,\theta_0)\psi=0\ , \tag{4}$$

and

$$U^2(k,z,\theta_0)=\epsilon_r(k,z)-\sin^2\theta_0>0\ . \tag{5}$$

The field solutions to the differential equation (4) can be expressed as an integral equation by using the one-dimensional Green's function[11] $\exp(ik\,|z-z'|\cos\theta_0)/(k\cos\theta_0)$,

$$\psi(z,k,\theta_0)=\psi_{\text{in}}+\frac{ik}{2\cos\theta_0}\int_{-\infty}^{\infty}\exp(ik\,|z-z'|\cos\theta_0)\times[\epsilon_r(k,z')-1]\psi(z',k,\theta_0)dz'\ , \tag{6}$$

where $\psi_{\text{in}}=\exp(ikz\cos\theta_0)$. An expression for the reflection coefficient $r(k,\theta_0)$ can be obtained from Eqs. (6) and (1) by applying the continuity of E_y at $z=0$,

$$r(k,\theta_0)=\frac{ik}{2\cos\theta_0}\int_0^L\exp(ikz\cos\theta_0)[\epsilon_r(k,z)-1]\times\psi(z,k,\theta_0)dz\ . \tag{7}$$

Equation (7) is an exact expression for $r(k,\theta_0)$ in terms of the relative dielectric permittivity and the electric field within the dielectric. If the dielectric region is electrically thin, i.e., for weak scattering, the following condition is satisfied,

$$kL\,|\epsilon_r(k,z)-1|\ll 1\ , \tag{8}$$

where L is the thickness of the region. Under this assumption Eq. (6) indicates that a reasonable approximation for the interior electric field amplitude is

$$\psi(z,k,\theta_0)\approx\psi_{\text{in}}(z,k,\theta_0) \tag{9}$$

and after substituting this approximation into the integral in Eq. (7), and assuming that the permittivity is lossless and dispersionless, $\epsilon_r(k,z)=\epsilon_r(z)$, then the Fourier transform of $r(k,\theta_0)$ with respect to k yields the inversion algorithm

$$[\epsilon_r(z)-1]=\frac{4\cos^2\theta_0}{i}\times\left[\frac{1}{2\pi}\int_{-\infty}^{\infty}\frac{r(k,\theta_0)}{k}\exp(-i2kz\cos\theta_0)dk\right]\ , \tag{10}$$

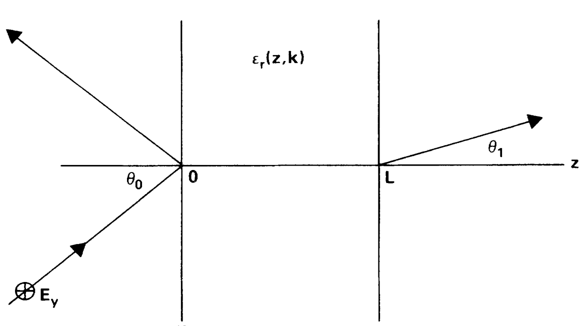

FIG. 1. Physical model for scattering of plane waves from an inhomogeneous dielectric region.

which is equivalent to the Born approximation[3,4] and provides a simple and direct procedure for reconstructing the dielectric profile $\epsilon_r(z)$ from $r(k,\theta_0)$. However, the condition imposed by Eq. (8) restricts its utility to small values of k or weak reflections.

The radius of convergence of the inversion algorithm in k space is increased by applying the method of multiple scales. In order to accomplish this, the differential equation (4) for the electric field within the dielectric region is expressed in terms of the electromagnetic path length $s(z,\theta_0)$ in the dielectric region,

$$s(z,\theta_0)=\int_0^z U(z',\theta_0)dz' ,\quad s(0,\theta_0)=0,\quad s(L,\theta_0)=s_L . \tag{11}$$

Equation (11) is the Liouville transformation[12] between z, which is a fast variable, and s, which is a slow variable; note that the function $U(z,\theta_0)$, Eq. (5), is assumed to be piecewise continuous. The differential equation (4) for the electric field within the slab can now be expressed in s space as

$$\frac{d^2\psi}{ds^2}+g(z,\theta_0)\frac{d\psi}{ds}+k^2\psi=0 , \tag{12}$$

where

$$g(z,\theta_0)=\frac{1}{U^2(z,\theta_0)}\frac{dU}{dz}=\frac{d}{ds}\{\ln[U(z(s),\theta_0)]\} . \tag{13}$$

The renormalized inversion theory of I and II assumed that the function $g(z,\theta_0)$ was a continuous and slowly varying function of position z. Under this assumption, an approximate solution for ψ was constructed by the perturbation technique of multiple scales which is a form of renormalization theory. An equivalent solution can be readily obtained by converting Eq. (12) to an integral equation for the wave amplitude in s space by using the Green's function $\exp(ik\,|s-s'|)/k$,

$$\psi(s,k)=\exp(iks)+\frac{i}{2k}\int_0^{s_L}\exp(ik\,|s-s'|)\frac{d}{ds'}\times\{\ln[U(s')]\}\frac{d\psi}{ds'}ds' , \tag{14}$$

where the θ_0 dependence has been absorbed within s, so that the reflection coefficient can be expressed as

$$r(k)=\frac{i}{2k}\int_0^{s_L}\exp(iks)\frac{d}{ds}\{\ln[U(s)]\}\frac{d\psi}{ds}ds . \tag{15}$$

As an initial approximation for ψ in the interior of the dielectric slab, we let

$$\psi(s,k)\simeq\psi_{\rm in}(s,k)=\exp(iks) . \tag{16}$$

Substituting Eq. (16) into Eq. (15) and taking the Fourier transform of $r(k,\theta_0)$ over k space yields an ordinary differential equation for the dielectric profile in s space,

$$-\frac{1}{4}\frac{d}{ds}\{\ln[U(S)]\}=\frac{1}{2\pi}\int_{-\infty}^{\infty}r(k,\theta_0)\exp(-2iks)dk =R(2s) , \tag{17}$$

which is readily integrated to give the effective dielectric profile

$$U(s)=U(0)\exp\left[-2\int_0^{2s}R(t)dt\right] . \tag{18}$$

This generalizes Eq. (31) of I by using the effective dielectric profile at non-normal incidence, $U(s)$. Equation (18) results from an effective summation of the secular terms in the perturbation solution of Eq. (12). Thus it is a field renormalization obtained by requiring energy conservation for the electromagnetic field within the dielectric region.

It has been demonstrated by several calculations that this algorithm has a larger radius of convergence in k space than the Born approximation. However, the penalty paid for this advantage is that the dielectric reconstruction is defined in s space. The dielectric profile function in geometric z space is obtained by expanding the Liouville transformation (11) as a Maclaurin series,

$$s(z,\theta_0)=\begin{cases} U(0,\theta_0)z+\dfrac{1}{4}\dfrac{1}{U(0,\theta_0)}\left[\dfrac{d\epsilon_r}{dz}\right]_{z=0}z^2+\cdots , & z>0 \\ z\cos\theta_0, \quad z<0 . \end{cases} \tag{19}$$

Applying reversion of series to Eq. (19) yields

$$z=z(s,\theta_0) =\frac{1}{[\epsilon_r(0)-\sin^2\theta_0]^{1/2}}[s-\tfrac{1}{4}g(0,\theta_0)s^2]+\cdots, \quad z>0 . \tag{20}$$

Equation (20) indicates that $z\approx s/\cos\theta_0$ if the dielectric profile is continuous $[\epsilon_r(0)=1]$ and slowly varying $[g(0,\theta_0)\ll 1]$. If the slab thickness L is known in geometric space, this linear transformation from s to z space can be used to reconstruct the dielectric profile in geometric space. If L is not known, the reconstruction contains an unknown multiplicative constant.[2]

If the profile is discontinuous $[\epsilon_r(0)\neq 1]$ but slowly varying away from the discontinuity, Eq. (20) provides a correction to reconstruct the profile in z space. Thus it is important to be able to estimate the magnitude of the discontinuity at the origin. In the next section we will analyze this problem by using a singular perturbation technique. The asymptotic behavior of the profile as $s \to \infty$ can be obtained from Eqs. (17) and (18). Using the assumption that the region $z \le 0$ is a homogeneous half-space, i.e., the left-hand side of Eq. (17) is 0 for $z \le 0$, and taking the Fourier transform of Eq. (17) (with $t \equiv 2s$) which introduces the Dirac delta function into Eq. (17), Eq. (18) reduces to (with $k=0$)

$$\lim_{s \to \infty} U(s) = U(0)\exp[-2r(0,\theta_0)] \ . \tag{21}$$

A demonstration of this asymptotic behavior for $U(0) \ne 1$ is given in example 2; note that $r(0,\theta_0)$ might not be 0.

Equation (18) is a renormalized solution of the inverse-scattering problem that is equivalent to a second-order regular perturbation approximation of the exact GLM theory. The term involving the first derivative in Eq. (12) is eliminated by the change of variable[12]

$$\psi(s,k,\theta_0) = \frac{v(s,k,\theta_0)}{[\epsilon_r(z) - \sin^2\theta_0]^{1/4}} \ . \tag{22}$$

This transformation assumes that the functional form of $\epsilon_r(z)$ is known; in general this *a priori* information is not available. By using the method of multiple scales it is possible to obtain this transformation without knowing the explicit form of $\epsilon_r(z)$. Substituting Eq. (22) into Eq. (12) yields a Schrödinger-type equation for $v(s,k)$ in s space,

$$\frac{d^2}{ds^2}v + [k^2 - q(s)]v = 0 \ , \tag{23}$$

where the effective potential $q(s)$ is defined by

$$q(s) = \frac{1}{2}\frac{d}{ds}\left[\frac{d}{ds}\ln[U(s)]\right] + \frac{1}{4}\left[\frac{d}{ds}\ln[U(s)]\right]^2 \ . \tag{24}$$

The mathematically exact relationship between $q(s)$ and $r(k)$ is provided by GLM theory[1,2,13,14]; the basic equations can be conveniently obtained by considering a time-dependent formulation of the scattering problem. The Fourier transform $\Psi(s,t)$ of $\psi(s,k)$ satisfies the time-dependent wave equation

$$\frac{\partial^2}{\partial s^2}\Psi(s,t) - \frac{\partial^2}{\partial t^2}\Psi(s,t) - q(s)\Psi(s,t) = 0 \ , \tag{25}$$

where t is the time variable with the velocity of light $c \equiv 1$. In free space the incident plane wave for the time dependent equation (25) is represented by the unit impulse

$$\Psi_{\rm in}(s,t) = \delta(s-t) \ , \tag{26}$$

which produces the reflected transient or characteristic function

$$R(s+t) = \frac{1}{2\pi}\int_{-\infty}^{\infty} r(k)\exp[-ik(s+t)]dk \ . \tag{27}$$

Due to causality,

$$R(s) = 0 \quad \text{for } s < 0 \ , \tag{28}$$

i.e., a reflected transient is not produced until the incident pulse has interacted with the inhomogeneous medium. It is possible to relate the wave amplitude $\Psi(s,t)$ in the inhomogeneous region with the wave amplitude $\Psi_0(s,t)$ in the free-space region by the linear transformation

$$\Psi(s,t) = \Psi_0(s,t) + \int_{-\infty}^{\infty} K(s,z')\Psi_0(z',t)dz' \ , \tag{29}$$

where

$$\Psi_0(s,t) = \delta(s-t) + R(s+t) \ . \tag{30}$$

From physical considerations we know that $\Psi(s,t)$ is a rightward-moving transient, so that

$$\Psi(s,t) = 0 \quad \text{for } s > t \ . \tag{31}$$

Thus $K(s,t)=0$ for $t > s$. Substituting expression (30) into Eq. (29) and using Eqs. (28) and (31) yields the integral equation

$$K(s,t) + R(s+t) + \int_{-t}^{s} K(s,z')R(z'+t)dz' = 0, \quad s > t \tag{32}$$

which is Kay's version[2] of the Gel'fand-Levitan-Marchenko integral equation. Substituting representation (29) into the wave equation (25) shows that the function $K(s,t)$ satisfies a differential equation of the same form as Eq. (25) for the wave amplitude $\Psi(s,t)$ if the following conditions are imposed:

$$K(s,-s) = 0 \ , \tag{33}$$

$$2\frac{d}{ds}K(s,s) = q(s) \ . \tag{34}$$

Thus if the integral equation (32) can be solved for the function $K(s,t)$, then Eq. (34) yields the mathematically exact solution to this inverse-scattering problem. Various methods for solving Eq. (32) are possible; especially important are those where the scattering data are represented by rational reflection coefficients $r(k)$ since these are physically interesting and have wide ranges of application.[15]

Integral equation (32) can be solved iteratively for $K(s,t)$ by considering the integral to be a perturbation term in the equation and introducing the ordering parameter ρ, so that Eq. (32) becomes

$$K(s,t) + R(s+t) + \rho\int_{-t}^{s} K(s,z')R(z'+t)dz' = 0, \quad s > t \ . \tag{35}$$

Expanding $K(s,t)$ in a regular perturbation series,

$$K(s,t) = \sum_{n=1}^{\infty} \rho^n K_n(s,t) \ , \tag{36}$$

leads to the second-order perturbation solution for $q(s)$,[8]

$$q(s) = -2\frac{d}{ds}[R(2s)] + 4[R(2s)]^2 \ , \tag{37}$$

when $\rho \equiv 1$. It can be shown[16] that the expression for the dielectric profile, Eq. (18), is the exact analytic solution of Eq. (24) if approximation (37) is used for $q(s)$ and an appropriate integrating factor is used to solve this Riccati equation. This result is equivalent to the zero-order renormalized solution. The first-order approximation for the electric field can be obtained by substituting Eq. (17) into Eq. (14) and evaluating the integral to obtain

$$\Psi(s,k)=\exp(iks)\left[1-\frac{1}{2}\ln\frac{U(s)}{U(0)}\right]; \tag{38}$$

this process can be iterated. Since the asymptotic form of the solution of Eq. (22) is known to be[12]

$$\Psi(s,k)=\exp(iks)\exp\left[-\frac{1}{2}\ln\frac{U(s)}{U(0)}\right], \tag{39}$$

the iterative approach yields the correct series expansion for the solution if $|\frac{1}{2}\ln[U(s)/U(0)]|<1$.

RENORMALIZED INVERSION THEORY FOR DISCONTINUOUS PROFILES

In I and II the function $g(z,\theta_0)$ in Eq. (13) was assumed to be a continuous and slowly varying function of position z; under this assumption an approximate solution for $\epsilon_r(z)$ was constructed by a perturbation technique of multiple scales. Here we consider a discontinuous dielectric profile such that $g(z,\theta_0)$ is not assumed to be a slowly varying function in the neighborhood of the dielectric discontinuity; this inverse problem is cast as a singular perturbation problem and solved by the method of multiple scales.

Equation (12) for the electric field within the dielectric slab can be rewritten in the form of a singular perturbation problem[17]

$$\sigma^2\left[\frac{d^2\psi}{d\eta^2}+\frac{d}{d\eta}\{\ln[U(s)]\}\frac{d\psi}{d\eta}\right]+\psi=0, \tag{40}$$

where $\eta=s/s_L$ is a dimensionless spatial parameter and the perturbation parameter $\sigma=1/ks_L\ll 1$. Thus the present analysis is applicable to high-frequency data since $s_L>L$ and $k\gg 1$.

The local behavior of the electromagnetic field near the discontinuity will be determined by the high-frequency Born approximation. In order to perform the multiple-scale analysis of Eq. (40) two independent variables are introduced,

$$\eta_0=\eta \quad\text{and}\quad \eta_1=\frac{\eta_0}{\sigma}; \tag{41}$$

η_0 is a slow variable and corresponds to the outer variable of boundary-layer theory and η_1 is a fast variable and corresponds to the inner variable. The differential operators defined in Eq. (40) are now replaced by partial differential operators

$$\frac{d}{d\eta}=\frac{\partial}{\partial\eta_0}+\frac{1}{\sigma}\frac{\partial}{\partial\eta_1}\equiv D_0+\left[\frac{1}{\sigma}\right]D_1, \tag{42}$$

$$\frac{d^2}{d\eta^2}=\frac{\partial^2}{\partial\eta_0^2}+\frac{2}{\sigma}\frac{\partial^2}{\partial\eta_0\partial\eta_1}+\frac{1}{\sigma^2}\frac{\partial^2}{\partial\eta_1^2}$$
$$\equiv D_0^2+\left[\frac{2}{\sigma}\right]D_0D_1+\left[\frac{1}{\sigma^2}\right]D_1^2.$$

Substituting these expressions into Eq. (40) yields the following partial differential equation for ψ,

$$D_1^2\psi+\psi+\sigma[2D_0D_1\psi+D_0(\ln U)D_1\psi]+\sigma^2[D_0^2\psi+D_0(\ln U)D_0\psi]=0, \tag{43}$$

and a solution for this equation is sought in the form

$$\psi=\psi_0(\eta_0,\eta_1)+\sigma\psi_1(\eta_0,\eta_1)+\sigma^2\psi_2(\eta_0,\eta_1)+\cdots. \tag{44}$$

Substituting Eq. (44) into Eq. (43) and equating corresponding powers of the perturbation parameter yields a coupled system of partial differential equations,

$$\sigma^0:\ (D_1^2+1)\psi_0=0, \tag{45}$$

$$\sigma^1:\ (D_1^2+1)\psi_1=-[2D_0D_1\psi_0+D_0(\ln U)D_1\psi_0], \tag{46}$$

$$\sigma^2:\ (D_1^2+1)\psi_2=-[2D_0D_1\psi_1+D_0(\ln U)D_1\psi_1]-[D_0^2\psi_0+D_0(\ln U)D_0\psi_0]. \tag{47}$$

The general solution of the zero-order equation (45) is

$$\psi_0=A_0(\eta_0)\exp(i\eta_1)+B_0(\eta_0)\exp(-i\eta_1), \tag{48}$$

which has the form of a harmonic oscillation with constant coefficients on the fast scale η_1. Substituting the zero-order solution (48) into the first-order equation (46) for ψ_1 yields

$$(D_1^2+1)\psi_1=-i[2D_0A_0+A_0D_0(\ln U)]\exp(i\eta_1)+\text{c.c.}, \tag{49}$$

where c.c. denotes complex conjugate of the first term; Eq. (49) has the form of a driven harmonic oscillator with frequency one. The forcing terms on the right-hand side are in resonance with this frequency and will lead to divergent behavior of ψ_1/ψ_0 as $\eta\to\infty$. In order to conserve energy, this secular growth is denied by equating the arbitrary coefficients of the resonant terms to zero. Thus by denying secular growth in the first-order correction for ψ, the functional forms of the coefficients of the zero-order solution on the slow scale are determined from the condition

$$2D_0A_0+A_0D_0(\ln U)=0, \tag{50}$$

whose solution is

$$A_0(\eta_0)=\frac{\alpha_0}{[U(\eta_0)]^{1/2}}, \tag{51}$$

where α_0 is an integration constant. The general solution of the first-order equation (46) is now given by

$$\psi_1=A_1(\eta_0)\exp(i\eta_1)+B_1(\eta_0)\exp(-i\eta_1). \tag{52}$$

The variable coefficients in this solution are determined by denying those terms which lead to secular growth in the equation for the second-order correction. The general solution through first order for the electric field is

$$\psi=\alpha_0\exp(i\eta_1)\left[1-\frac{i\sigma}{2}\int_0^{\eta_0}q(t)dt\right][U(\eta_0)]^{-1/2}+\text{c.c.}, \tag{53}$$

where

$$\alpha_0=[1+r(k,\theta_0)][U(0)]^{1/2} ,$$

as determined by the boundary condition at $z=0$.

Since $\eta_1=\eta_0/\sigma$, Eq. (53) reveals that the electric field is a highly oscillatory function of η_0. The high-frequency solution represented by Eq. (53) only makes a significant contribution to $r(k,\theta_0)$ in the neighborhood of the origin, as can be demonstrated by considering the dimensionless form of Eq. (15) for the reflection coefficient. Writing this as a function of σ yields

$$r(\sigma)=\frac{i\sigma}{2}\int_0^1 \exp\left[\frac{i\eta_0}{\sigma}\right]\frac{d}{d\eta_0}[\ln U(s_L,\eta_0)]\frac{d\psi}{d\eta_0}d\eta_0 , \tag{54}$$

where

$$\frac{d\psi}{d\eta_0}=\alpha_0\exp\left[\frac{i\eta_0}{\sigma}\right]\left[\frac{i}{\sigma}\frac{1}{[U(\eta_0)]^{1/2}}-\frac{1}{2}\frac{1}{U^{3/2}}\frac{dU}{d\eta_0}\right.$$
$$-\frac{i\sigma}{2}\left[q(\eta_0)\frac{1}{[U(\eta_0)]^{1/2}}\right.$$
$$\left.\left.-\frac{1}{2}\frac{1}{U^{3/2}}\frac{dU}{d\eta_0}\right]\int_0^{\eta_0}q(t)dt\right] . \tag{55}$$

Substituting (55) into (54) yields

$$r(\sigma)=\frac{i}{2}\int_0^1\alpha_0\exp\left[\frac{2i\eta_0}{\sigma}\right]\frac{d}{d\eta_0}[\ln U(s_L,\eta_0)]\left[\frac{i}{[U(\eta_0)]^{1/2}}-\frac{1}{2}\frac{\sigma}{[U(\eta_0)]^{3/2}}\frac{dU}{d\eta_0}+O(\sigma^2)\right]d\eta_0 . \tag{56}$$

As $\sigma\to 0$, the higher-order powers of σ can be neglected and Eq. (54) reduces to

$$r(\sigma)=-\tfrac{1}{2}\int_0^1\frac{\alpha_0\exp\left[\dfrac{2i\eta_0}{\sigma}\right]}{[U(\eta_0)]^{1/2}}\frac{d}{d\eta_0}[\ln U(s_L,\eta_0)]d\eta_0 . \tag{57}$$

The exponential term in Eq. (57) oscillates rapidly in the high-frequency limit ($\sigma\to 0$) so that, if the integrand is integrable, the contributions to $r(k,\theta_0)$ from adjacent subintervals within the dielectric effectively cancel; this observation follows from the Riemann-Lebesgue lemma,[10]

$$\lim_{\sigma\to 0} r(\sigma)=\lim_{\sigma\to 0}\int_a^b f(t)\exp(it/\sigma)dt=0 . \tag{58}$$

Rewriting Eq. (57) in the original variables with $t=2s$, we obtain

$$r(k)=-\tfrac{1}{2}\int_0^{2s_L}\frac{\alpha_0\exp(ikt)}{\sqrt{U}(t)}\frac{d}{dt}(\ln U)dt . \tag{59}$$

Taking the Fourier transform of Eq. (59), we obtain

$$\int_{-\infty}^{\infty} r(k)\frac{e^{ikt}}{2\pi}dk=-\tfrac{1}{2}\int_{-\infty}^{\infty}\frac{e^{ikt'}dk}{2\pi}\left[\int_0^{2s_L}\frac{\alpha_0\exp(ikt)}{\sqrt{U}(t)}\frac{d}{dt}(\ln U)dt\right]$$
$$\simeq-\frac{1}{2}\frac{1}{\sqrt{U}}\frac{d}{dt'}(\ln U) , \tag{60}$$

for $\alpha_0\approx 1$. Taking the high-frequency limit $k\to\infty$ and using Eq. (58), the right-hand side of Eq. (60) also goes to 0. Physically, this means that the profile U obtained from Eq. (60) will have no meaningful solutions from high-frequency reflection data away from the origin $t>0$. Thus the high-frequency inversion algorithm considered here can only provide the correct local behavior for dielectric profiles. Equation (57) is analogous to the Born approximation used in Eq. (15) in the renormalized inversion algorithm for the continuous profile. The dielectric profile in s space can now be calculated by using an equation of the same form as Eq. (18) except that for the discontinuous profile, $R(0)\neq 1$. The multiple-scales analysis has summed the terms of the high-frequency perturbation solution of the inverse-scattering problem and included local behavior of the discontinuous profile by using the high-frequency Born approximation.

The fact that $R(0)\neq 1$ suggests that a discontinuous profile is present and also provides the means for the renormalization of this inverse-scattering theory. The asymptotic behavior of $U(s)$, Eq. (21), reveals that the dielectric discontinuity $U(0)$ "propagates" in s space, which induces a bias in the reconstructed profile, as shown in example (ii) Fig. 4. With the assumption that the reflection data were obtained from a finite slab of known thickness, the effective permittivity $U(s)$ approaches its free-space value as $s\to\infty$. A bias in the reconstruction due to this propagation of the discontinuity $U(0)$ can be eliminated with the transformation to z space by reversion of series.

EXAMPLES

The renormalized inversion theory will be applied to two examples that illustrate, first, the second-order perturbation solution of the GLM equation starting with a rational $r(k)$ and, second, the approximate solution of the GLM equation starting with numerical data generated by the solution of a direct-scattering problem. The reflection data of Fig. 3 and the dielectric profiles of Figs. 2, 4 and 5 have been reproduced directly from computer plots; computer artifacts have not been removed.

(i) The reflection coefficient $r(k)$ is produced by plane waves normally incident upon a semi-infinite inhomogeneous electron plasma whose positive background makes a negligible contribution to $r(k)$. In the absence of a static magnetic field and electron collisions in the physical model of Fig. 1 with $L \to +\infty$, the relative permittivity has the form[18]

$$\epsilon_r(k,z) = \left[1 - \frac{1}{k^2} q(z) \right] , \tag{61}$$

where the profile function $q(z)$ is proportional to the electron density. In this case the time-independent Helmholtz equation (4) can be transformed directly into the time-independent Schrödinger equation in z space. The reflection coefficient is represented by a rational function of k with two poles on the unit circle in the complex k plane; these are designated "Butterworth poles,"

$$r(k) = r(k,\theta_0=0) = \frac{-k_1 k_2}{(k-k_1)(k-k_2)} ,\qquad k_1 = \frac{1}{\sqrt{2}}(1-i), \quad k_2 = -\bar{k}_1 . \tag{62}$$

This inverse problem has been solved by using the exact GLM theory[19] to obtain the profile function

$$q(z) = \begin{cases} 0, & z \le 0 \\ \dfrac{4}{(1+\sqrt{2}z)^2}, & z \ge 0 \end{cases} \tag{63}$$

which has the Maclaurin expansion

$$q(z) = 4[1 - 2\sqrt{2}z + 3(\sqrt{2}z)^2 + \cdots], \quad z \ge 0 . \tag{64}$$

The high-frequency behavior of the fields near the discontinuity at $z=0$ provides the approximate solution $\tilde{q}(z)$. Using the approximation (9) in (7) gives

$$r(k) = \frac{i}{2k} \int_{-\infty}^{\infty} \exp(i2kz)\tilde{q}(z)dz , \tag{65}$$

so that using (62) and taking the Fourier transform of (63),

$$\tilde{q}(z) = r_1 \exp(-i2k_1 z) + r_2 \exp(-i2k_2 z) , \tag{66}$$

where r_1 and r_2 are the residues of $r(k)$. The Maclaurin expansion of $\tilde{q}(z)$ is

$$\tilde{q}(z) = \tilde{q}(0) + \left[\frac{d\tilde{q}}{dz} \right]_{z=0} z + \cdots , \tag{67}$$

so that for the pole configuration of (62),

$$\tilde{q}(z) = 4 - 8\sqrt{2}z + 8z^2 + \cdots . \tag{68}$$

The correct local behavior of $q(z)$ is obtained up to first order in z; thus the application of singular perturbation theory has provided a mathematical justification for the *ad hoc* results of Ge *et al.*[20]

Turning points for the local solutions of the differential equation will occur when $\epsilon_r = 1 - q(z)/k^2 = 0$. Using Eq. (68) for $\tilde{q}(z)$ up to first order in z, the turning point at $k=1$ occurs at $z=(1/2)\sqrt{2}$ and at $k=2$ occurs at $z=0$; examples of reconstructed profiles and their associated turning points are shown in Fig. 2.

(ii) The reflection coefficient data are numerically generated by solving the direct problem for scattering from an *a priori* assumed linear gradient in the permittivity,

$$\epsilon_r(z) = \begin{cases} (a+bz) & |z| \le L , \\ 1 \text{ elsewhere} , \end{cases} \tag{69}$$

where $a=2.5$, $b=1.0$, and $L=2.0$. The reflection coefficient in the inhomogeneous region obeys the Riccati equation [I, Eq. (33)]

$$\frac{dr}{dz}(z,k) = \frac{-ik}{2}[\epsilon_r(z)(1+r)^2 - (1-r)^2] \quad |z| \le L . \tag{70}$$

A fourth-order Runge-Kutta method was used to solve this differential equation with the dielectric profile, Eq. (69), in order to obtain the complex reflection data of Fig. 3. The reflection coefficient displays strong reflections over a bandwidth $kL \approx 25\times 2$ that represents several orders of magnitude in wave-number space and is much larger than that allowed by the Born approximation. The discrete numerical data for $r(k)$ were used in the inversion algorithm, Eqs. (58) and (18), to obtain the profile in s space, Fig. 4. Information about the limiting behavior, $R(s) \to R(0) = 2.5$ as $s \to \infty$, and reversion of series produced the reconstruction in z space, Fig. 5.

DISCUSSION

A renormalized solution that is based upon the exact inversion theories by Gel'fand, Levitan, and Marchenko

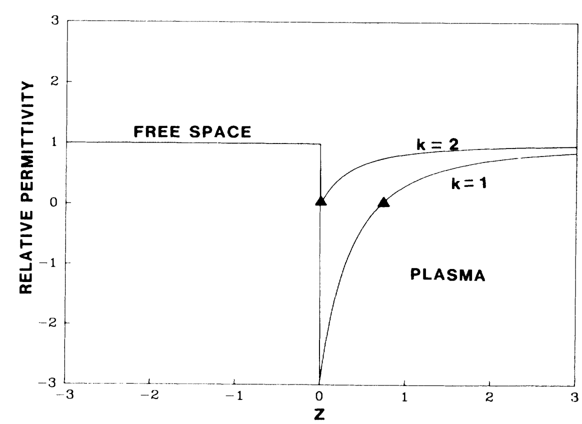

FIG. 2. Local behavior of the dielectric profiles $\epsilon_r(k,z)$ reconstructed from the rational $r(k)$ of example (i). Turning points are indicated by Δ.

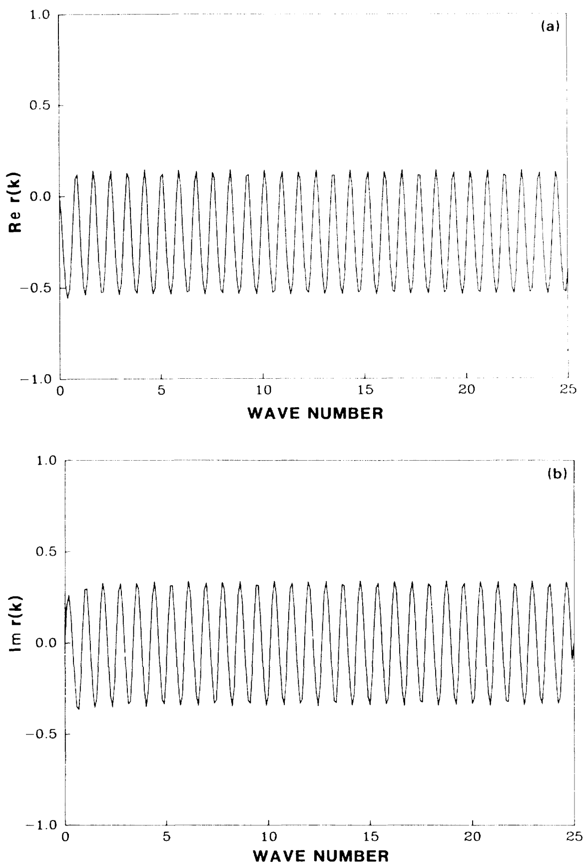

FIG. 3. Numerical reflection coefficient data generated by solution of the direct-scattering problem of example (ii): (a) real part of $r(k)$, (b) imaginary part of $r(k)$.

has been developed by using a multiple-scales analysis. Our previous theory for the inverse-scattering problem for inhomogeneous, continuously varying regions has been extended to include discontinuities in the dielectric permittivity. A singular perturbation method has been used to obtain a uniformly valid expression for the electric field within the dielectric region. The advantage of

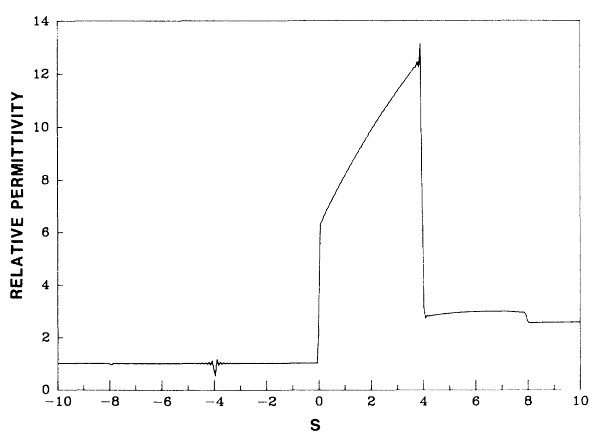

FIG. 4. Dielectric profile reconstructed in s space from the data of Fig. 3.

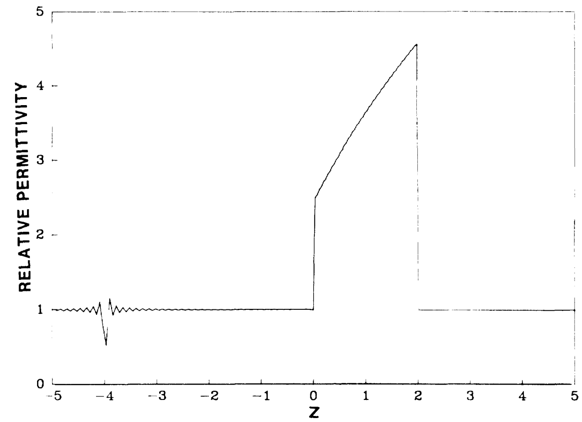

FIG. 5. Dielectric profile reconstructed in z space from the s-space data for the profile in Fig. 4.

the multiple-scales analysis of the interior electric field is that it rigorously indicates the dielectric region over which the weak-scattering or high-frequency approximation is valid. Furthermore, it is an effective renormalization technique that is physically motivated by the requirement of energy conservation and that allows a systematic investigation of the various scales associated with the inverse problem.

The singular perturbation method for the solution of the inverse problem associated with the electromagnetic reflection data from a discontinuous dielectric region utilizes the high-frequency Born approximation to determine the magnitude of the discontinuity in the neighborhood of the origin. However, in applying this approximation information about the correct dielectric structure away from the origin is lost. This conclusion is supported by the Riemann-Lebesque lemma. In order to reconstruct the interior region of the dielectric slab, the low-frequency data can be used. With the assumption that the interior dielectric region is a slowly varying function of position, the interior reconstruction can be performed with Eq. (17). The reconstructed profiles can then be combined to provide a complete solution for the reconstruction of the discontinuous dielectric profile. The singular perturbation methods used for reconstructing discontinuous profiles have also provided the reconstruction of profiles with turning points.

By using the Riemann-Lebesgue lemma to evaluate the integral of Eq. (57), the solution of this inverse problem required only general *a priori* information about the profile, i.e., that its logarithmic gradient be absolutely integrable. Equation (57) could be evaluated by other methods, e.g., integration by parts, which may not work at stationary points in the dielectric region. The Riemann-Lebesgue lemma does not require specific *a priori* information about stationary points since $r(\sigma)$ still goes to zero, although possibly more slowly.

The renormalization was actually carried out in electromagnetic path length s space; the dielectric permittivity function was transformed to geometric z space by numerical reversion of series. For certain types of dependence of the dielectric permittivity function on k, e.g., Eq. (59), analytic transformations can be obtained, so that the Helmholtz equation (4) is transformed directly to a Schrödinger equation (22) in geometric z space; otherwise the Liouville transformation (11) must be used. This transformation assumes that the functional form and extent of the relative permittivity $\epsilon_r(k,z)$ are known; the multiple-scales method does not require *a priori* knowledge of the functional form of $\epsilon_r(k,z)$ which would be needed for an analytic transformation between z and s spaces. Furthermore, if the Liouville transformation (10) is a monotonic function of z and independent of k, the reflection coefficients in z and s spaces are identical. These renormalized solutions are equivalent to the second-order perturbation solution of the GLM equation in s space. The Fourier transform of the time-independent Helmholtz equation is simply related to the plasma wave equation, which has physically meaningful solutions for continuous spectra.[14,15]

If the reflection coefficient is represented by a rational function $r(k)$ of the wave-number k, then it is possible to relate the functional form of the reconstructed profile $q(z)$ with the pole-zero configuration of $r(k)$. In general, the "smoothness" of $q(z)$ increases as the number of poles, N, of $r(k)$ increases; several examples of this behavior have been given previously.[21] In addition, pole-zero configurations are restricted to "allowed" regions of the complex k plane, which are determined by physical conditions, e.g., $|r(k)|^2 \leq 1$. Thus the first-order agreement of the Maclaurin expansion for the exact $q(z)$, Eq. (64), with the approximate $\tilde{q}(z)$, Eq. (68), is due to the two-pole representation for $r(k)$, since the conditions on the solution $K(s,t)$ of Eq. (32) will depend on $R(0)$ and $R'(0)$.

The type and number of scaling parameters needed for renormalization were determined by the characteristics of the scattering data and by *a priori* information built into the inversion theory. The ordering parameter ρ was used for the regular perturbation analysis of the GLM integral equation, the fast and slow scales for smoothly varying profiles were distinguished by the logarithmic gradient of the dielectric profile γ and the local behavior of the electromagnetic field near a discontinuity by the high-frequency parameter σ. An inversion theory for strong reflections from several discontinuities will require many different scales.

[1]R. G. Newton, in *Proceedings of the Conference on Inverse Scattering: Theory and Application,* edited by J. B. Bednar *et al.* (SIAM, Philadelphia, 1983), pp. 1–74.

[2]I. Kay, Report No. EM-74, Institute of Mathematical Sciences, New York University, 1955 (unpublished); Commun. Pure Appl. Math. **13**, 371 (1960); See also I. Kay and H. E. Moses, *Inverse Scattering Papers: 1955-1963* (Math. Sci. Press, Brookline, Mass., 1982).

[3]A. J. Devaney, Opt. Lett. **7**, 111 (1982).

[4]W. Tabbara, IEEE Trans. Antennas Propag. **27**, 241 (1979).

[5]Lord Rayleigh, Proc. R. Soc. London, Ser. A **93**, 565 (1917).

[6]H. D. Ladouceur, and A. K. Jordan, J. Opt. Soc. Am. A **2**, 1916 (1985).

[7]H. D. Ladouceur, and A. K. Jordan, Proc. Inverse Opt. II **558**, 47 (1985).

[8]H. E. Moses, Phys. Rev. **102**, 559 (1956); see also Ref. 2.

[9]M. Nayfeh, *Perturbation Methods* (Wiley, New York, 1973), pp. 228–307.

[10]E. T. Whittaker and G. N. Watson, *A Course in Modern Analysis* (Cambridge University Press, London, 1952), p. 172.

[11]K. Chadan and P. C. Sabatier, *Inverse Problems in Quantum Scattering Theory* (Springer-Verlag, New York, 1977), p. 231.

[12]R. Bellman, *Perturbation Techniques in Mathematics, Engineering and Physics* (Dover, New York, 1972), pp. 80-114.

[13]J. H. Rose, M. Cheney and B. DeFacio, J. Math. Phys. **25**, 2995 (1984).

[14]R. G. Newton, Phys. Rev. A **31**, 3305 (1985).

[15]P. C. Sabatier, in *Proceedings of the Conference on Inverse Scattering: Theory and Applications,* edited by J. B. Bednar *et al.* (SIAM, Philadelphia, 1983), pp. 75–99.

[16]J. Hirsch, Opt. Acta **26**, 1273 (1979).

[17]C. M. Bender and S. A. Orzag, *Advanced Mathematical Methods for Scientists and Engineers* (McGraw-Hill, New York, 1978), p. 325.

[18]L. M. Brekhovskikh, *Waves in Layered Media* (Academic, New York, 1960), p. 188.

[19]A. K. Jordan and H. N. Kritikos, IEEE Trans. Antennas Propag. **21**, 909 (1974); **21**, 737(E) (1974).

[20]D. B. Ge, D. L. Jaggard and H. N. Kritikos, IEEE Trans. Antennas Propag. **31**, 804 (1983).

[21]A. K. Jordan and S. Ahn, Proc. IEE **126**, 945 (1979).